Luminescent Thin Films

DOI: 10.1002/anie.201305648

Highly Luminescent Thin Films of the Dense Framework $^3_\infty[EuIm_2]$ with Switchable Transparency Formed by Scanning Femtosecond-Pulse Laser Deposition**

Dieter Fischer, Larissa V. Meyer, Martin Jansen, and Klaus Müller-Buschbaum**

Abstract: *Highly luminescent switchable thin films of the dense framework $^3_\infty[EuIm_2]$ were deposited by a scanning laser ablation technique using a femtosecond laser. The films can be controlled in terms of film thickness and amount of material deposited such that the material properties of the bulk material are retained on the nanometer scale. Polycrystalline films are formed that can be switched between transparent at visible light and nontransparent at UV light due to the intrinsic luminescence of the hybrid material, expanding the concept of smart films. The new femtosecond pulsed laser deposition method also provides a novel approach for coatings with framework compounds and coordination polymers.*

The large variety of physical and chemical properties of coordination polymers and metal–organic frameworks (MOFs) have brought them into the focus of research.[1–4] Photophysical effects contribute to the multifunctionality of these inorganic–organic hybrid materials, including effective luminescence by the organic chromophores as well as metal-based luminescence processes.[5–8] Possible applications of luminescent coordination polymers range from solid lighting to sensing and sensor applications.[9–11] Apart from the bulk material, coatings of both thin and thick films are interesting for sensing and as membranes, and have recently become the center of research on coordination polymers and MOFs.[12] In work on thin films, the possibility of switching glass coatings between transparent and nontransparent has attracted attention and led to the terms smart films or switchable films, which typically change from transparent to opaque upon regulated voltage.[13] Switching of thin films by use of luminescence is a rare feature, found for example, for poly-oxometallates,[14] and has not yet been observed for framework compounds or MOFs. Established techniques for the deposition of thin films include spin-coating, dip-coating, casting processes, solvothermal self-assembly techniques, and layer-by-layer deposition from solution.[15] However, gas-phase-related processes like chemical vapor deposition (CVD) and physical vapor deposition (PVD) would be favorable for the creation of functionalized thin films with high purity. Of the multitude of PVD methods, pulsed laser deposition (PLD) is preferable over thermal evaporation. Possible reasons are provided by several intrinsic properties of coordination polymers: they are crystalline solids with low vapor pressure that have unknown gas-phase species and limited thermal stability. The PLD technique[16] allows adjustment of the energy transfer into the material by the appropriate choice of process parameters, for example, wavelength, laser power, pulse duration, and repetition rate. Thus, PLD has been used as an alternative to the spray-coating of organic films.[17] However, during ablation the organic and polymeric materials partially decompose and the resulting films are rich in defects. To overcome this problem, matrix-assisted pulsed laser evaporation from frozen polymer solutions at concentrations < 5 wt % has been considered.[18]

The dense framework[19] europium(II) imidazolate $^3_\infty[EuIm_2]$, $(Im^- = C_3N_2H_3^-)$[20] was studied, as it exhibits intense efficient photoluminescence with a quantum yield (QY) exceeding 60 % and high thermal stability, the latter being a prominent feature of metal imidazolates and zeolitic imidazolate frameworks (ZIFs).[21] It marks an excellent model system for the proof of principle of PLD coating for thin films made up of luminescent coordination polymers.

Here we describe the physical vapor deposition of a highly luminescent dense europium imidazolate framework creating thin layers 100–500 nm thick by a new method in which a femtosecond laser beam[22] is used to ablate the hybrid material in a vacuum chamber (Figure 1 and the Supporting Information). To the best of our knowledge, this is the first example of the use of ultrashort pulsed lasers to create films of frameworks or coordination polymers and the first controlled PVD process for such compounds as well. We call the new technique scanning femto-PLD since it combines the PLD concept with laser scanner technology and a femtosecond laser system under ultra-high-vacuum conditions.

The reproducible creation of thin films by femto-PLD that have the initial framework structure $^3_\infty[EuIm_2]$ was confirmed by X-ray diffraction and luminescence properties. At a thickness of 100–150 nm, the films are transparent for visible light and can be switched to be nontransparent by excitation with UV light due to the intrinsic luminescence of the films. To the best of our knowledge, this is also the first example of a switchable film of framework and MOF compounds that utilizes luminescence. Further evidence that the framework $^3_\infty[EuIm_2]$ is retained is given by its intrinsic turquoise emission. The switching of transparency is achieved by

[*] L. V. Meyer, Prof. Dr. K. Müller-Buschbaum
Institut für Anorganische Chemie, Universität Würzburg
Am Hubland, 97074 Würzburg (Germany)
E-mail: k.mueller-buschbaum@uni-wuerzburg.de
Homepage: http://www.mueller-buschbaum.anorganik.chemie.uni-wuerzburg.de/
Dr. D. Fischer, Prof. Dr. M. Jansen
Max-Planck-Institut für Festkörperforschung
Heisenbergstrasse 1, 70569 Stuttgart (Germany)
E-mail: m.jansen@fkf.mpg.de

[**] This work was supported by the Deutsche Forschungsgemeinschaft.
Supporting information for this article is available on the WWW under http://dx.doi.org/10.1002/anie.201305648.

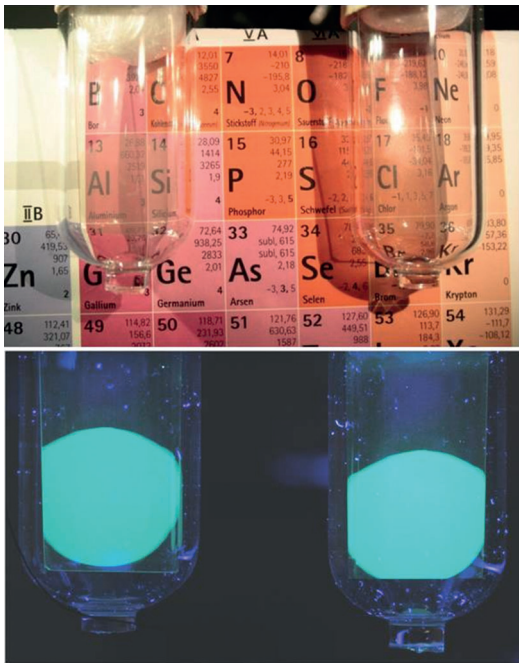

Figure 1. Switchable films of europium(II) imidazolate with a thickness of 100 nm (left) and 150 nm (right) on sapphire substrates (0001): transparent under visible light (top) and nontransparent under UV light (bottom) due to the photoluminescence of the films.

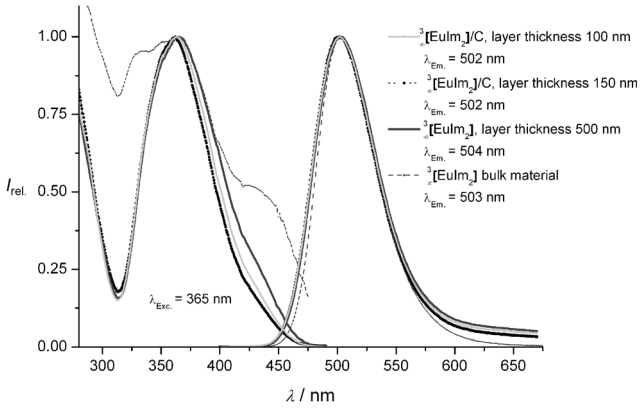

Figure 2. Excitation and emission spectra of films of $^3_\infty$[EuIm$_2$] and $^3_\infty$[EuIm$_2$]/C with varying film thickness and comparison to the spectra of the bulk material (λ_{exc} = 365 nm).

a combination of the intrinsic emission and reflection of incoming and emitted light at the surface of the film particles. No special rotation angle of the film and the coated substrate surface are required for the observation of transparency switching.

The photoluminescence of $^3_\infty$[EuIm$_2$] has been previously investigated on the bulk material.[20] It is bright and efficient, as europium in its divalent state allows 5d–4f transitions for emission. Since the energy of the 5d states is lowered by ligand- and crystal-field splitting, the emission is in the visible range at short edge of wavelengths for a green light impression, giving turquoise–green light. In contrast to Ln^{III} (4f–4f) luminescence, Eu^{II} does not suffer from parity-forbidden transitions[23] and gives strong emission and a more efficient light absorption than trivalent lanthanides.[24] Since for Eu^{II} the 5d orbitals are included, the energy levels depend on the chemical surrounding and the chemical bonding, which marks a major difference to trivalent lanthanides. Accordingly, photoluminescence changes upon variation of the coordination sphere, bonding character, and crystal structure. Therefore, $^3_\infty$[EuIm$_2$] with divalent europium was chosen, as the photoluminescence can be used as additional evidence that the framework is deposited without modification. This "fingerprint" works well even for thin films of a thickness of 100 nm. Both excitation and emission due to 4f→5d and 5d→4f transitions remain unchanged relative to the bulk material (see Figure 2 and Figure S4). The results of photoluminescence spectroscopy prove that $^3_\infty$[EuIm$_2$] can be successfully used for femtosecond laser ablation and recrystallizes on sapphire substrates.

The films were fully characterized by X-ray powder diffraction, X-ray photoelectron spectroscopy (XPS), photoluminescence (PL) spectroscopy, scanning electron microscopy (SEM), and energy-dispersive X-ray (EDX) spectroscopy. The gas-phase species were investigated by mass spectrometry including matrix-assisted laser desorption/ionization time-of-flight (MALDI-TOF) mass spectrometry.

Unexpectedly, polycrystalline films of $^3_\infty$[EuIm$_2$] were obtained by the new PLD process. X-ray powder diffraction corroborates the crystal structure of the dense framework with no crystalline side phases observed (Figure 3). First weak powder patterns can be observed at layer thicknesses of $\geq$100 nm and they exhibit all major reflections of the framework. The crystal domain sizes are about 250 nm. X-ray powder diffraction also proves that the material recrystallizes on the substrate; cooled substrates give amorphous material, which upon heating at 200 °C gives the crystalline domains observed.

In order to have processible targets for PLD, the framework was compressed to a pellet prior to ablation. The material was also mixed with graphite to dilute the luminescent framework, to increase the adherence of the brittle framework particles, and to achieve conductivity. Coating using the femto-PLD method proved successful for pure $^3_\infty$[EuIm$_2$] as well as $^3_\infty$[EuIm$_2$]/graphite mixtures. Films made from both targets show transparency and switching upon excitation.

It is remarkable that graphite is deposited as amorphous carbon from samples prepared from mixed imidazolate/graphite targets. The difference between carbon and the polycrystalline $^3_\infty$[EuIm$_2$] coating leads to the question of how the layer is formed. In order to investigate the deposition of both carbon and the europium imidazolate, we examined representative films with Raman spectroscopy. Raman bands of amorphous carbon are found at about 1350 to 1550 cm^{-1}[25] in the $^3_\infty$[EuIm$_2$]/C films, and weak Eu–N Raman bands of $^3_\infty$[EuIm$_2$] are at about 200 cm^{-1} (Figure S1).[20] The deposited films were further characterized by SEM (Figure 4) and EDX spectroscopy (Figure S2). These investigations show thicknesses on the order of 100–150 nm for the given laser power and deposition time for the transparent films. The surface topography shows particleswith an extension of 50 nm–2 μm and a height of 20–100 nm which are not related to the size of

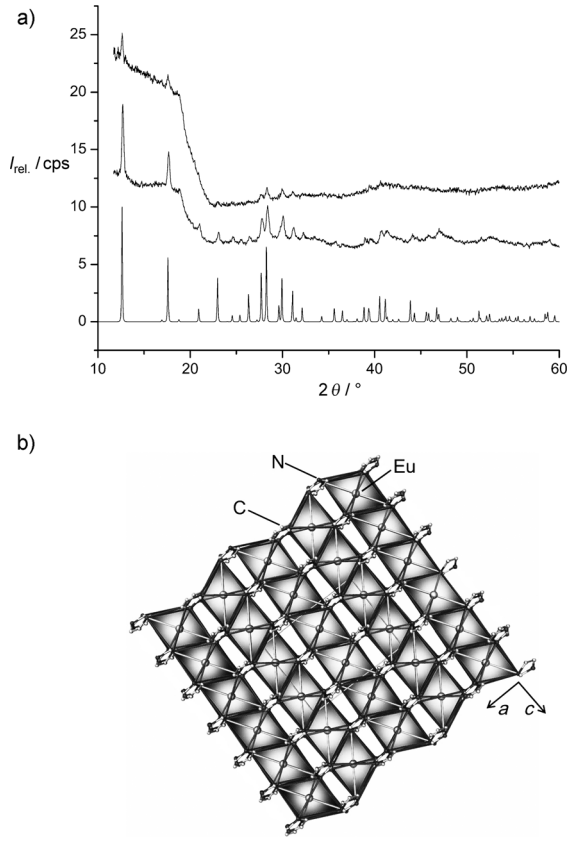

Figure 3. a) Powder X-ray diffraction patterns of deposited films ($^3_\infty$[EuIm$_2$]/C, 150 nm thick (top); $^3_\infty$[EuIm$_2$], 500 nm thick (middle)), and a simulated pattern calculated from single-crystal structure data (bottom); $Cu_{K\alpha}$ radiation. b) Crystal structure of $^3_\infty$[EuIm$_2$].

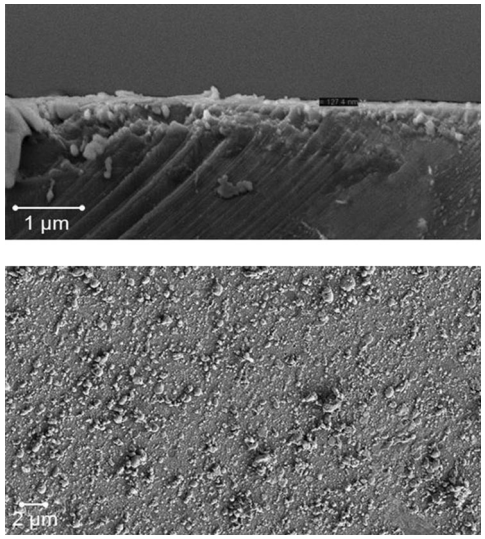

Figure 4. SEM visualization (top: side view; bottom: view of the surface) of $^3_\infty$[EuIm$_2$]/C films on sapphire substrates (detector resolution 1.9 nm at 1 kV).

the crystal domain. This topography might hint at the material transport process.

Typically, lanthanides show high oxophilicity. We therefore checked by X-ray photoelectron spectroscopy (XPS) whether the framework $^3_\infty$[EuIm$_2$] would form stable thin films that retain the properties of the bulk material attributed to the presence of divalent europium. Reference data from thin EuO films[26] and even intermetallic phases[27,28] show that europium is indeed divalent with a minor surface oxidation to Eu^{III}, as was also observed for EuO films (Figure S3).[26]

To identify gas-phase species, mass spectrometry was carried out on the gas atmosphere during the deposition experiments. For $m/z < 100$ only fragments smaller than an imidazolate ring were detected and not the ligand itself. This indicates either total fragmentation or transport of fragments larger than the detection range through the gas phase. As it is unlikely that the ligand reforms after total fragmentation, we exclude it from the mechanism leading to successful ablation. MALDI-TOF(+) mass spectrometry was carried out on the deposited films for clarification. It shows fragments in two mass regions with significant signals at $m/z = 151$ to 218 as well as 337 to 382. Whilst the lowest mass can be identified as europium atoms, $m/z = 218$ corresponds to one Eu atom and one imidazolate ligand. Larger masses indicate that also larger fragments are brought into the gas phase by laser ablation. At the moment, the ablation process cannot be clearly identified and will be further investigated. As the laser pulse and thus the energy source of the femto-PLD is shorter in duration than any vibration, the excitation from vibrations leading to cleavage of bonds is limited compared to other methods like thermal procedures. Femtosecond pulses result in the transfer of photon energy directly to the electrons of the target. In view of this, it is remarkable that $^3_\infty$[EuIm$_2$] does not survive thermal evaporation in an effusion cell. Instead of deposition, decomposition of $^3_\infty$[EuIm$_2$] is observed in the crucible of the cell at $T > 480\,°C$. Therefore thermal activation is not suitable. In contrast, it is possible to form coatings of substrates with our new PLD method by using ultrashort pulsed lasers, and thus functionalized films of dense frameworks can be prepared in a controlled fashion, as shown for the switchable nanometer-scale films of $^3_\infty$[EuIm$_2$]. With this method properties of the bulk material are retained. Thus, the femto-PLD method seems to be an attractive method for the formation of films of inorganic–organic hybrid materials through gas-phase deposition that cannot be deposited by other methods.

To summarize, the dense framework $^3_\infty$[EuIm$_2$] was successfully deposited as luminescent thin films by scanning femto-PLD onto sapphire substrates. The deposition is achieved by a pulsed femtosecond laser. In contrast, thermal evaporation using an effusion cell or an excimer laser does not lead to deposition but decomposition of $^3_\infty$[EuIm$_2$]. Thin films of variable thickness can be created by variation of laser power and deposition time giving homogenous coatings. The framework $^3_\infty$[EuIm$_2$] is deposited as amorphous or polycrystalline material depending on the substrate temperature, and its material properties and crystal structure are retained. The films switch between transparent for visible light and nontransparent upon excitation with UV light due to the intrinsic framework luminescence. Luminescence and the accompanying switch from transparent to nontransparent films can thereby expand the research area of smart films and point to future directions for coordination polymers. To the best of our

knowledge, this is the first example utilizing an ultrashort pulsed laser for coating with a framework compound. Moreover, physical vapor deposition is uncommon due to the low volatility and low thermal stability of MOFs and coordination polymers. The results presented demonstrate possible gas-phase transport, which can be used in addition to coating techniques by liquid phases. Even the formation of crystalline films is possible for materials like the switchable framework films presented here.

Experimental Section

$^3_\infty$[EuIm$_2$] was prepared by a modified version of the original synthesis (oxidation of europium metal by imidazole according to Ref. [20]). Instead of a ligand melt, electride-induced reaction in liquid ammonia was selected (according to the procedure described in Ref. [29]). For experimental details, please see the Supporting Information.

Since $^3_\infty$[EuIm$_2$] is sensitive to moisture and air, the samples were handled under argon atmosphere or vacuum. To obtain processible targets of $^3_\infty$[EuIm$_2$], the pure luminescent framework, as well as mixtures with added graphite (50%) were used to form pellets. Therefore, pure $^3_\infty$[EuIm$_2$] powder was pressed at a pressure of 10 tons to form a pellet with a diameter of 13 mm (thickness ca. 3 mm). A second pellet was prepared from a 1:1 mixture of $^3_\infty$[EuIm$_2$]/graphite under the same conditions.

The experimental setup of the scanning femto-PLD instrumentation is illustrated in Figure 5.[22] The laser target consists of a pressed pellet of $^3_\infty$[EuIm$_2$] or $^3_\infty$[EuIm$_2$]/graphite, which rotates at a fixed angle in a vacuum chamber and is ablated by a horizontal line scan of a pulsed laser beam which is focused on the target surface. The evaporated europium imidazolate is directly deposited onto a sapphire substrate at room temperature ((0001) orientation, epitaxial polishing, CrysTec GmbH) for 5–7 h; operating distance 15 cm.

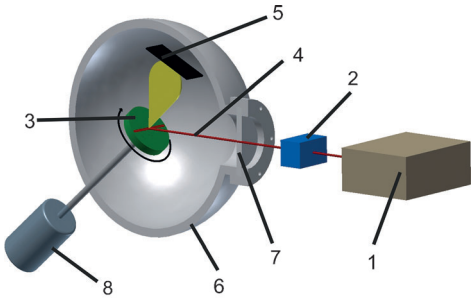

Figure 5. Illustration of the scanning femto-PLD setup (1: laser, 2: scanner, 3: target, 4: laser beam, 5: substrate, 6: vacuum chamber, 7: optical window, 8: motor).

The vacuum conditions and gas phase ($0.8–2.5 \times 10^{-7}$ mbar) were monitored by appropriate pressure sensors and a quadrupole mass spectrometer (QME 220, Pfeiffer Vacuum GmbH). The target was rotated by a motor outside the chamber at a fixed rotation speed of 0.0233 s^{-1}. The laser beam of the 442-fs pulsed laser emitting at a wavelength of 516 nm and with a laser power ranging between 0.2 and 0.3 W (energy per pulse of 0.2–0.3 mJ at 1 kHz; femtoRegen IC-375, High-Q-Laser GmbH, Hohenems) was guided through a set of flat mirrors, a beam expander, and a galvanometer mirror box (HurryScan25, Scanlab AG, Puchheim) with convenient software control (Samlight, Scaps GmbH, Deisenhofen) into the vacuum chamber. The beam, focused onto the target with a spot size of 0.04 mm, was scanned (50 mm s^{-1}) as a horizontal line over the whole target surface (for further details on the method see Ref. [22]). Film thicknesses of 100 to 500 nm were determined by SEM techniques combined with qualitative XRF spectroscopy.

Received: July 1, 2013
Published online: December 2, 2013

Keywords: coordination polymers · luminescence · metal–organic frameworks · pulsed laser deposition · thin films

[1] a) S. Kitagawa, M. Kondo, *Bull. Chem. Soc. Jpn.* **1998**, *71*, 1739–1753; b) C. Serre, F. Millange, C. Thouvenot, M. Nogues, G. Marsolier, D. Louer, G. Ferey, *J. Am. Chem. Soc.* **2002**, *124*, 13519–13526; c) J. L. C. Rowsell, O. M. Yaghi, *Microporous Mesoporous Mater.* **2004**, *73*, 3–14.

[2] a) O. M. Yaghi, G. Li, H. Li, *Nature* **1995**, *378*, 703–706; b) S. Kitagawa, R. Kitaura, S. Noro, *Angew. Chem.* **2004**, *116*, 2388–2430; *Angew. Chem. Int. Ed.* **2004**, *43*, 2334–2375; c) G. Férey, C. Mellot-Draznieks, C. Serre, F. Millange, *Acc. Chem. Res.* **2005**, *38*, 217–225; d) S. Ma, H.-C. Zhou, *Chem. Commun.* **2010**, *46*, 44–53; e) S. Meek, J. Greathouse, M. Allendorf, *Adv. Mater.* **2011**, *23*, 249–267.

[3] a) S. L. James, *Chem. Soc. Rev.* **2003**, *32*, 276–288; b) K. Sumida, D. Rogow, J. A. Mason, T. M. McDonald, E. D. Bloch, Z. R. Herm, T.-H. Bae, J. R. Long, *Chem. Rev.* **2012**, *112*, 724–781; c) M. P. Suh, H. J. Park, T. K. Prasad, D.-W. Lim, *Chem. Rev.* **2012**, *112*, 782–835; d) L. J. Murray, M. Dincă, J. R. Long, *Chem. Soc. Rev.* **2009**, *38*, 1294–1314; e) A. U. Czaja, N. Trukhan, U. Müller, *Chem. Soc. Rev.* **2009**, *38*, 1284–1293; f) J.-R. Li, J. Sculley, H.-C. Zhou, *Chem. Rev.* **2012**, *112*, 869–932; g) J.-R. Li, R. J. Kuppler, H.-C. Zhou, *Chem. Soc. Rev.* **2009**, *38*, 1477–1504.

[4] a) A. Lan, K. Li, H. Wu, D. Olson, T. J. Emge, W. Ki, M. Hong, J. Li, *Angew. Chem.* **2009**, *121*, 2370–2374; *Angew. Chem. Int. Ed.* **2009**, *48*, 2334–2338; b) A. M. Shultz, O. K. Farha, J. T. Hupp, S. T. Nguyen, *J. Am. Chem. Soc.* **2009**, *131*, 4204–4205; c) R. E. Morris, X. Bu, *Nat. Chem.* **2010**, *2*, 353–361.

[5] a) M. D. Allendorf, C. A. Bauer, R. K. Bhakta, R. J. T. Houk, *Chem. Soc. Rev.* **2009**, *38*, 1330–1352; b) J. Rocha, L. D. Carlos, F. A. Almeida Paz, D. Ananias, *Chem. Soc. Rev.* **2011**, *40*, 926–940; c) Y. Cui, Y. Yue, G. Qian, B. Chen, *Chem. Rev.* **2012**, *112*, 1126–1162.

[6] a) X.-L. Qi, R. B. Lin, Q. Chen, J. B. Lin, J.-P. Zhang, X.-M. Chen, *Chem. Sci.* **2011**, *2*, 2214–2218; b) Y.-N. Wu, F. Li, W. Zhu, J. Cui, C.-A. Tao, C. Lin, P. M. Hannam, G. Li, *Angew. Chem.* **2011**, *123*, 12726–12730; *Angew. Chem. Int. Ed.* **2011**, *50*, 12518–12522.

[7] a) Q.-Y. Liu, Y.-L. Wang, N. Zhang, Y.-L. Jiang, J.-J. Wie, F. Luo, *Cryst. Growth Des.* **2011**, *11*, 3717–3720; b) K. Liu, H. You, Y. Zheng, G. Jia, L. Zhang, Y. Huang, M. Yang, Y. Song, H. Zhang, *CrystEngComm* **2009**, *11*, 2622–2628; c) H. Zhang, N. Li, C. Tian, T. Liu, F. Du, P. Lin, Z. Li, S. Du, *Cryst. Growth Des.* **2012**, *12*, 670–678; d) P. Falcaro, S. Furukawa, *Angew. Chem.* **2012**, *124*, 8557–8559; *Angew. Chem. Int. Ed.* **2012**, *51*, 8431–8433; e) D. F. Sava, L. E. S. Rohwer, M. A. Rodriguez, T. M. Nenoff, *J. Am. Chem. Soc.* **2012**, *134*, 3983–3986.

[8] a) K. Müller-Buschbaum, S. G. Torres, P. Larsen, C. Wickleder, *Chem. Mater.* **2007**, *19*, 655–659; b) C. J. Höller, M. Mai, C. Feldmann, K. Müller-Buschbaum, *Dalton Trans.* **2010**, *39*, 461–468; c) C. J. Höller, P. R. Matthes, M. Adlung, C. Wickleder, K. Müller-Buschbaum, *Eur. J. Inorg. Chem.* **2012**, 5479–5484; d) P. R. Matthes, C. J. Höller, M. Mai, J. Heck, S. J. Sedlmaier, S. Schmiechen, C. Feldmann, W. Schnick, K. Müller-Buschbaum, *J. Mater. Chem.* **2012**, *22*, 10179–10187; e) J.-C. Rybak, L. V. Meyer, J. Wagenhöfer, G. Sextl, K. Müller-Buschbaum, *Inorg. Chem.* **2012**, *51*, 13204–13213.

[9] a) L. E. Kreno, K. Leong, O. K. Farha, M. Allendorf, R. P. Van Duyne, J. T. Hupp, *Chem. Rev.* **2012**, *112*, 1105 – 1125; b) Y. Li, S. Zhang, D. Song, *Angew. Chem.* **2013**, *125*, 738 – 741; *Angew. Chem. Int. Ed.* **2013**, *52*, 710 – 713; c) Y. Xiao, Y. Cui, Q. Zheng, S. Xiang, G. Qian, B. Chen, *Chem. Commun.* **2010**, *46*, 5503 – 5505; d) B. Zhao, X.-Y. Chen, P. Cheng, D.-Z. Liao, S.-P. Yan, Z.-H. Jiang, *J. Am. Chem. Soc.* **2004**, *126*, 15394 – 15395.

[10] a) W.-G. Lu, L. Jiang, X.-L. Feng, T.-B. Lu, *Inorg. Chem.* **2009**, *48*, 6997 – 6999; b) Z.-Z. Lu, R. Zhang, Y.-Z. Li, Z.-J. Guo, H.-G. Zheng, *J. Am. Chem. Soc.* **2011**, *133*, 4172 – 4174; c) B. Chen, Y. Yang, F. Zapata, G. Lin, G. Qian, E. B. Lobkovsky, *Adv. Mater.* **2007**, *19*, 1693 – 1696; d) J. An, C. M. Shade, D. A. Chengelis-Czegan, S. Petoud, N. L. Rosi, *J. Am. Chem. Soc.* **2011**, *133*, 1220 – 1223; e) S. Liu, Z. Xiang, Z. Hu, X. Zheng, D. Cao, *J. Mater. Chem.* **2011**, *21*, 6649 – 6653.

[11] a) B. Chen, L. Wang, Y. Xiao, F. R. Fronczek, M. Xue, Y. Cui, G. Qian, *Angew. Chem.* **2009**, *121*, 508 – 511; *Angew. Chem. Int. Ed.* **2009**, *48*, 500 – 503; b) G. Lu, J. T. Hupp, *J. Am. Chem. Soc.* **2010**, *132*, 7832 – 7833; c) Y. Takashima, V. M. Martinez, S. Furukawa, M. Kondo, S. Shimomura, H. Uehara, M. Nakahama, K. Sugimoto, S. Kitagawa, *Nat. Commun.* **2011**, *2*, 168; d) Z. Xie, L. Ma, K. E. de Krafft, A. Jin, W. Lin, *J. Am. Chem. Soc.* **2010**, *132*, 922 – 923; e) Z. Guo, H. Xu, S. Su, J. Cai, Dang, S. Xiang, G. Qian, H. Xhang, M. O'Keeffe, B. Chen, *Chem. Commun.* **2011**, *47*, 5551 – 5553.

[12] a) A. Bétard, R. A. Fischer, *Chem. Rev.* **2012**, *112*, 1055 – 1083; b) O. Shekhah, J. Liu, R. A. Fischer, C. Wöll, *Chem. Soc. Rev.* **2011**, *40*, 1081 – 1106.

[13] a) X. H. Xia, J. P. Tu, J. Zhang, X. H. Huang, X. L. Wang, W. K. Zhang, H. Huang, *Electrochem. Commun.* **2009**, *11*, 702 – 705.

[14] a) B. Wang, Z.-D. Yin, L.-H. Bi, L.-X. Wu, *Chem. Commun.* **2010**, *46*, 7163 – 7165; b) F. Amano, D. Li, B. Ohtani, *J. Electrochem. Soc.* **2011**, *158*, K42 – K46.

[15] a) S. Hermes, F. Schröder, R. Chelmowski, C. Wöll, R. A. Fischer, *J. Am. Chem. Soc.* **2005**, *127*, 13744 – 13745; b) O. Shekhah, H. Wang, S. Kowarik, F. Schreiber, M. Paulus, M. Tolan, C. Sternemann, F. Evers, D. Zacher, R. A. Fischer, C. Wöll, *J. Am. Chem. Soc.* **2007**, *129*, 15118 – 15119; c) J. Gascon, S. Aguado, F. Kapteijn, *Microporous Mesoporous Mater.* **2008**, *113*, 132 – 138; d) Y. S. Li, F. Y. Liang, H. G. Bux, W. S. Yang, J. Caro, *J. Membr. Sci.* **2010**, *354*, 48 – 54; e) P. Horcajada, C. Serre, D. Grosso, C. Boissière, S. Perruchas, C. Sanchez, G. Férey, *Adv. Mater.* **2009**, *21*, 1931 – 1935; f) S. Bundschuh, O. Kraft, H. K. Arslan, H. Gliemann, P. G. Weidler, C. Wöll, *Appl. Phys. Lett.* **2012**, *101*, 101910 – 101914; g) Y. Yoo, H.-K. Jeong, *Cryst. Growth Des.* **2010**, *10*, 1283 – 1288; h) H. K. Arslan, O. Shekhah, J. Wohlgemuth, M. Franzreb, R. A. Fischer, C. Wöll, *Adv. Funct. Mater.* **2011**, *21*, 4228 – 4231; i) S. Hermes, D. Zacher, A. Baunemann, C. Wöll, R. A. Fischer, *Chem. Mater.* **2007**, *19*, 2168 – 2173.

[16] J. Perrière, E. Millon, V. Cracuin in *Pulsed Laser Deposition of Thin Films* (Ed.: R. Eason), Wiley, Hoboken, **2007**.

[17] a) J. Schou in *Functionalized Nanoscale Materials, Devices and Systems* (Eds.: A. Vaseashta, I. N. Mihailescu), Springer Science & Business Media, B.V., Dordrecht, **2008**, pp. 248 – 256; b) D. Vak, S.-S. Kim, J. Jo, S.-H. Oh, S.-I. Na, J. Kim, D.-Y. Kim, *Appl. Phys. Lett.* **2007**, *91*, 081102.

[18] a) A. Piqué, *Appl. Phys. A* **2011**, *105*, 517 – 528; b) A. Gutierrez-Llorente, G. Horowitz, R. Perez-Casero, J. Perriere, J. L. Fave, A. Yassar, C. Sant, *Org. Electron.* **2004**, *5*, 29 – 34.

[19] A. K. Cheetham, C. N. R. Rao, *Science* **2007**, *318*, 58 – 59.

[20] A. Zurawski, M. Mai, D. Baumann, C. Feldmann, K. Müller-Buschbaum, *Chem. Commun.* **2011**, *47*, 496 – 498.

[21] a) H. Hayashi, A. P. Cote, H. Furukawa, M. O'Keefe, O. M. Yaghi, *Nat. Mater.* **2007**, *6*, 501 – 507; b) R. Banerjee, A. Phan, B. Wang, C. Knobler, H. Furukawa, M. O'Keeffe, O. Yaghi, *Science* **2008**, *319*, 939 – 943; c) D. W. Lewis, A. R. Ruiz-Salvador, A. Gomez, L. M. Rodriguez-Albelo, F.-X. Coudert, B. Slater, A. K. Cheetham, C. Mellot-Draznieks, *CrystEngComm* **2009**, *11*, 2272 – 2276; d) J. Cravillon, C. A. Schröder, R. Nayuk, J. Gummel, K. Huber, M. Wiebcke, *Angew. Chem.* **2011**, *123*, 8217 – 8221; *Angew. Chem. Int. Ed.* **2011**, *50*, 8067 – 8071; e) J. Cravillon, R. Nayuk, S. Springer, A. Feldhoff, K. Huber, M. Wiebcke, *Chem. Mater.* **2011**, *23*, 2130 – 2141; f) K. Müller-Buschbaum, *Z. Naturforsch. B* **2006**, *61*, 792 – 798; g) K. Müller-Buschbaum, F. Schönfeld, *Z. Anorg. Allg. Chem.* **2011**, *637*, 955 – 960; h) A. Zurawski, J.-C. Rybak, L. V. Meyer, K. Müller-Buschbaum, *Z. Anorg. Allg. Chem.* **2013**, *639*, 261 – 267.

[22] D. Fischer, G. F. de La Fuente, M. Jansen, *Rev. Sci. Instrum.* **2012**, *83*, 043901 – 043909.

[23] a) J.-C. Bünzli, S. V. Eliseeva in *Basics of Lanthanide Photophysics* (Eds.: P. Hänninen, H. Härmä), Springer, Berlin, **2010**; b) G. H. Dieke, *Spectra and energy levels of rare earth ions in crystals*, Interscience Publishers, New York, **1968**.

[24] a) J.-C. Bünzli, C. Piguet, *Chem. Soc. Rev.* **2005**, *34*, 1048 – 1077; b) K. Binnemans, *Chem. Rev.* **2009**, *109*, 4283 – 4374; c) S. V. Eliseeva, J.-C. Bünzli, *Chem. Soc. Rev.* **2010**, *39*, 189 – 227.

[25] a) P. K. Chu, L. Li, *Mater. Chem. Phys.* **2006**, *96*, 253 – 277; b) M. Marton, M. Vojs, E. Zdravecká, M. Himmerlich, T. Haensel, S. Krischok, M. Kotlár, P. Michniak, M. Veselý, R. Redhammer, *J. Spectrosc.* **2013**, 467079 – 467085.

[26] C. Caspers, M. Müller, A. X. Gray, A. M. Kaiser, A. Gloskovskii, C. S. Fadley, W. Drube, C. M. Schneider, *Phys. Status Solidi* **2011**, *1* – 3.

[27] C. Laubschat, B. Perscheid, W.-D. Schneider, *Phys. Rev. B* **1983**, *28*, 4342 – 4348.

[28] L. C. Gupta, E. V. Sampathkumaran, R. Vijayaraghavan, V. Prabhawalkar, P. D. Prabhawalkar, B. D. Padalia, *Phys. Rev. B* **1983**, *23*, 4283 – 4285.

[29] C. C. Quitmann, K. Müller-Buschbaum, *Angew. Chem.* **2004**, *116*, 6120 – 6122; *Angew. Chem. Int. Ed.* **2004**, *43*, 5994 – 5996.

